

Dynamical polarization processes in double quantum dots coupled in series

This article has been downloaded from IOPscience. Please scroll down to see the full text article.

2008 J. Phys.: Condens. Matter 20 275244

(<http://iopscience.iop.org/0953-8984/20/27/275244>)

View [the table of contents for this issue](#), or go to the [journal homepage](#) for more

Download details:

IP Address: 129.252.86.83

The article was downloaded on 29/05/2010 at 13:26

Please note that [terms and conditions apply](#).

Dynamical polarization processes in double quantum dots coupled in series

G Michałek and B R Bułka

Institute of Molecular Physics, Polish Academy of Sciences, ulica Mariana Smoluchowskiego 17, 60-179 Poznań, Poland

E-mail: grzechal@ifmpan.poznan.pl

Received 18 January 2008, in final form 21 May 2008

Published 13 June 2008

Online at stacks.iop.org/JPhysCM/20/275244

Abstract

The polarization processes in a system of double quantum dots coupled in series with electrodes are studied in the limit of sequential tunnelling. The Coulomb interactions of accumulated charges on both quantum dots and the competition between dot–dot and dot–electrode coupling are responsible for the non-monotonic filling of each dot, which leads to a change of the sign of the polarization as a function of bias voltage. We show that this dynamical switching polarization effect is common and observable in various multidot systems.

(Some figures in this article are in colour only in the electronic version)

1. Introduction

Electrical transport through double quantum dots (2QDs) systems have been recently widely studied both experimentally [1–8] and theoretically [9–15] because of their interesting physical properties like e.g. negative differential conductance, single-electron pump, Pauli spin blockade, singlet–triplet transitions, competition between the Kondo effect and the antiferromagnetic correlations between spins on the 2QDs, etc. Furthermore, the single-electron devices based on 2QDs can be used e.g. to build current standards, room temperature memory, thermometry and charge sensing devices [16]. It was also proposed to use 2QDs as quantum gates and the building blocks of future quantum computers [17–21]. In addition, it was pointed out that the charging of the QD and the occupation of a single-particle level can show some rather complex, non-monotonic behaviour as a function of gate voltage [22], deviating considerably from the standard Coulomb blockade (CB) picture: one-by-one filling. This complex behaviour originates from the competition between the dot–electrode coupling and the intrinsic energy scales of the QD, i.e. its charging energy and level spacing. It is worth noting, that one can also find non-monotonic filling of the energy levels (as a function of bias voltage) in 2QDs capacitively coupled in parallel [23]. The competition between dot–electrode coupling and Coulomb interaction should also play an important role in 2QDs coupled in series to the electrodes.

In this paper we will study transport properties of serially coupled 2QDs in a sequential tunnelling regime. We predict that in the system a new interesting phenomenon can occur,

which we call *dynamical polarization switching* (DPS). This is an inversion of the polarization of the system from the negative to the positive value (or vice versa) as a bias voltage rises. The non-monotonic occupation of QD has been recently studied by König and Gefen [24] and by Kostyrko and Bułka [25]. Both papers treat the electronic transport in the coherent regime. In the König and Gefen paper the non-monotonic filling is due to a change of the density of states and due to changes of the spectral weight near resonant transmission. Kostyrko and Bułka found, that non-monotonic filling occurs due to the pinning of the resonant level to the Fermi level.

The paper is organized as follows: in section 2 we describe the formalism used for calculation of current, an average occupation of a QD and polarization. The results of our computations are presented in section 3. First we show that for certain values of parameters the DPS effect can occur. Then we discuss the dependence of this effect on the macroscopic parameters of the device, such as capacitance and resistance. The symmetrical system is mainly considered, i.e. with equal couplings to the left and right electrodes as well as equal charging energies of both quantum dots. Afterwards we will discuss the origin of the DPS effect. In section 4 final remarks are given, where asymmetrical systems and the influence of gate voltages on DPS will also be discussed.

2. Description of the model and calculation of the electronic transport in sequential tunnelling regime

We consider a system (presented in figure 1), composed of two quantum dots connected in series with electrodes. We assume

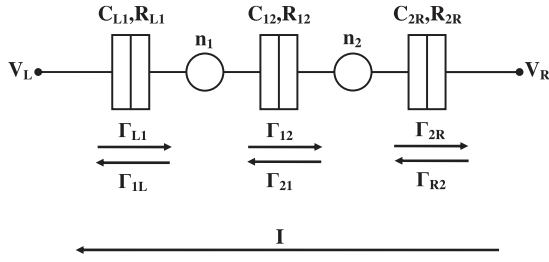


Figure 1. Schematic view of two serially coupled quantum dots. Each tunnel junction is characterized by two parameters: a capacitance C_{ij} and a resistance R_{ij} . V_L, V_R are voltages applied to the electrodes, Γ_{ij} are the effective tunnelling rates, and n_1, n_2 denote a number of additional electrons on first (QD1) and second (QD2) quantum dot.

that the electrodes are ideal and the potentials in the QDs are constant, so the voltage drops occur only on the tunnel barriers, which we have modelled by the resistances R_{ij} . From the Kirchhoff's laws, the voltage drops on the left, the middle and the right tunnel junctions are:

$$V_{L1} = -e \frac{C_{12} + C_{2R}}{C_s} n_1 - e \frac{C_{12}}{C_s} n_2 + \frac{C_{12} C_{2R}}{C_s} V_L - \frac{C_{12} C_{2R}}{C_s} V_R, \quad (1)$$

$$V_{12} = e \frac{C_{2R}}{C_s} n_1 - e \frac{C_{L1}}{C_s} n_2 + \frac{C_{L1} C_{2R}}{C_s} V_L - \frac{C_{L1} C_{2R}}{C_s} V_R, \quad (2)$$

$$V_{2R} = e \frac{C_{12}}{C_s} n_1 + e \frac{C_{L1} + C_{12}}{C_s} n_2 + \frac{C_{L1} C_{12}}{C_s} V_L - \frac{C_{L1} C_{12}}{C_s} V_R, \quad (3)$$

where C_{ij} is the capacitance of the junction ij ($ij = \{L1, 12, 2R\}$), $C_s = C_{L1} C_{12} + C_{L1} C_{2R} + C_{12} C_{2R}$, n_1 (n_2) denotes a number of additional electrons on QD1 (QD2) and e is an electron charge ($e < 0$). The charging energies of the dots are $E_1^{\text{ch}} = e^2(C_{12} + C_{2R})/C_s$, $E_2^{\text{ch}} = e^2(C_{L1} + C_{12})/C_s$ and the electrostatic coupling energy $E_{12}^{\text{ch}} = e^2 C_{12}/C_s$. The coupling energy E_{12}^{ch} is the change in the energy of one dot when an electron is added to the other dot [2].

In order to calculate transfer rates through the junctions the knowledge of the free energy of the system is needed. The free energy consists of the electrostatic energies of the charged capacitors in the system and the potential energies of the electrodes, and can be calculated for 2QDs system from the formula (see e.g. [26]):

$$F(n_1, n_2, n_L, n_R) = \frac{1}{2} (C_{L1} V_{L1}^2 + C_{12} V_{12}^2 + C_{2R} V_{2R}^2) - Q_L V_L - Q_R V_R, \quad (4)$$

where $Q_L = Q_{L1} + n_L e$ and $Q_R = -Q_{2R} + n_R e$ are the charges on the left and right electrode, respectively. n_R (n_L) is the number of electrons transferred from the left (right) electrode to the QD1 (QD2) and the charges on the capacitors C_{ij} are $Q_{ij} = C_{ij} V_{ij}$ ($ij = L1, 12, 2R$). The change of free energy due to electron tunnelling through the junction L1 from the left electrode to QD1 can be written as a difference

$$\Delta F_{L1}(n_1, n_2; n_1 + 1, n_2) = F_i(n_1, n_2, n_L, n_R) - F_f(n_1 + 1, n_2, n_L + 1, n_R), \quad (5)$$

where $F_i(n_1, n_2, n_L, n_R)$ and $F_f(n_1 + 1, n_2, n_L + 1, n_R)$ are the free energies of the initial and final states, respectively. One

can see from equations (4) and (5) that $\Delta F_{L1}(n_1, n_2; n_1 + 1, n_2)$ does not depend on n_L and n_R . An electron can be transferred through the junction (e.g. junction L1), when the corresponding free energy difference between initial (i) and final (f) states $\Delta F_{L1}(n_1, n_2; n_1 + 1, n_2) > 0$. The tunnelling rates through the junctions can be calculated on the basis of the method for a single QD with a continuous electronic density of states (DOS), described e.g. in the paper [27]. Applying the procedure to our system, one can obtain the following tunnelling rate for the transfer of one electron from the left electrode to the first QD through the junction L1:

$$\Gamma_{L1}(n_1, n_2; n_1 + 1, n_2) = \frac{\Delta F_{L1}(n_1, n_2; n_1 + 1, n_2)}{e^2 R_{L1}} \times \left[1 - \exp\left(-\frac{\Delta F_{L1}(n_1, n_2; n_1 + 1, n_2)}{k_B T}\right) \right]^{-1}, \quad (6)$$

where the tunnelling resistance R_{L1} of the junction L1 is given by $1/R_{L1} = 2\pi/\hbar |M_{L1}|^2 D_L D_1$ and D_L is DOS in the left electrode, while D_1 is DOS in QD1. It is assumed that DOS as well as matrix element M_{L1} (which describes transfer of an electron) are constant around the Fermi energy. Other tunnelling rates can be derived similarly. It is important to note that equation (6) is true when the electrons in the electrodes and on each dot are in thermal equilibrium even if the whole system of 2QDs is out of equilibrium. The assumption about thermal equilibrium on each quantum dot leads to conclusions that the charging energy E_i^{ch} of each QD is constant. Moreover the inelastic relaxation time τ_{in} on each QD is shorter than the time between successive tunnelling events $\tau_1 = e/I$ [28]. This relation implies that the corresponding resistances R_{ij} of the tunnel junctions ($ij = L1, 12, 2R$) are much larger than the quantum resistance $R_Q = h/2e^2$ and the electronic transport is dominated by incoherent, sequential tunnelling processes [29–31], whereas higher order processes (cotunnelling) are neglected. In addition temperature broadening is assumed to be strong, i.e. $h\Gamma_{ij} \ll k_B T$.

The state of the system at time t can be described by the probability $p(n_1, n_2; t)$ that the dots QD1 and QD2 have n_1 and n_2 additional electrons. The probability is normalized, so that condition $\sum_{n_1, n_2} p(n_1, n_2; t) = 1$ is fulfilled. The time evolution of the probability $p(n_1, n_2; t)$ depends on the tunnelling rates $\Gamma_{ij}(n_1, n_2; n'_1, n'_2)$. For each probability $p(n_1, n_2; t)$ one can write the master equation, which has the following form:

$$\frac{d}{dt} p(n_1, n_2; t) = - [\Gamma_{L1}(n_1, n_2; n_1 + 1, n_2) + \Gamma_{1L}(n_1, n_2; n_1 - 1, n_2) + \Gamma_{12}(n_1, n_2; n_1 - 1, n_2 + 1) + \Gamma_{21}(n_1, n_2; n_1 + 1, n_2 - 1) + \Gamma_{2R}(n_1, n_2; n_1, n_2 - 1) + \Gamma_{R2}(n_1, n_2; n_1, n_2 + 1)] p(n_1, n_2; t) + \Gamma_{L1}(n_1 - 1, n_2; n_1, n_2) p(n_1 - 1, n_2; t) + \Gamma_{1L}(n_1 + 1, n_2; n_1, n_2) p(n_1 + 1, n_2; t) + \Gamma_{12}(n_1 + 1, n_2 - 1; n_1, n_2) p(n_1 + 1, n_2 - 1; t) + \Gamma_{21}(n_1 - 1, n_2 + 1; n_1, n_2) p(n_1 - 1, n_2 + 1; t) + \Gamma_{2R}(n_1, n_2 + 1; n_1, n_2) p(n_1, n_2 + 1; t) + \Gamma_{R2}(n_1, n_2 - 1; n_1, n_2) p(n_1, n_2 - 1; t). \quad (7)$$

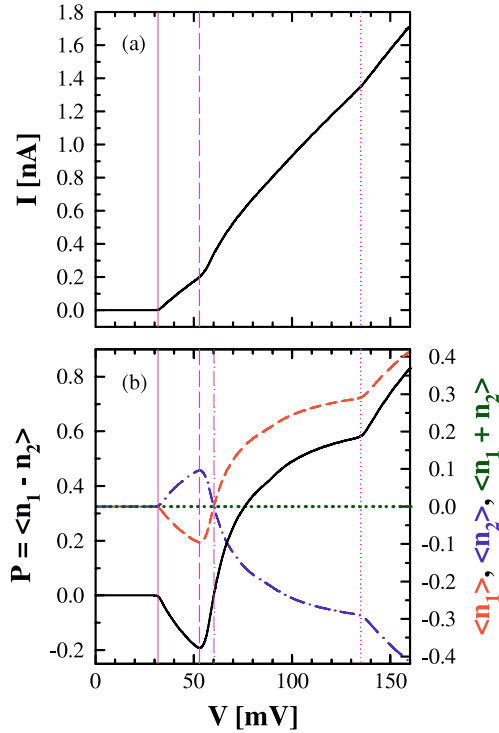


Figure 2. (a) Current, (b) polarization and charge accumulation plotted as a function of the bias voltage V . The charge $\langle n_1 \rangle$ and $\langle n_2 \rangle$ accumulated at QD1 and QD2 are presented as a dash and a dash-dot curve, the total charge accumulated in the system is $\langle n_1 + n_2 \rangle = 0$ (dot line), the polarization of the system $P = 2\langle n_1 \rangle$ (solid curve). The parameters are: $R_{L1} = R_{2R} = 10 \text{ M}\Omega$, $R_{12} = 50 \text{ M}\Omega$, $C_{L1} = C_{2R} = 5 \text{ aF}$, $C_{12} = 2 \text{ aF}$, $V_L = 0$, $V_R = V$, $T \approx 2.32 \text{ K}$. Thin horizontal lines denote threshold voltages: $V_1^{\text{th}} \approx 32 \text{ mV}$ (solid), $V_2^{\text{th}} \approx 56 \text{ mV}$ (dash), and $V_3^{\text{th}} \approx 136 \text{ mV}$ (dot) and switch voltage $V^{\text{switch}} \approx 60 \text{ mV}$ (dash-dot).

In the stationary state, due to the current conservation rule, the average currents flowing through each junction are equal $I_{L1} = I_{12} = I_{2R} = I$, and:

$$I = -e \sum_{n_1, n_2} [\Gamma_{L1}(n_1, n_2; n_1 + 1, n_2) - \Gamma_{1L}(n_1, n_2; n_1 - 1, n_2)] p(n_1, n_2), \quad (8)$$

where the steady state probability $p(n_1, n_2)$ can be determined from equation (7) with the left-hand side equal to zero. In the steady state, the average value of any physical quantity X can be expressed by

$$\langle X \rangle = \sum_{n_1, n_2} X(n_1, n_2) p(n_1, n_2), \quad (9)$$

where $X(n_1, n_2)$ is defined in the 2D space of states $\{(n_1, n_2)\}$.

3. Anomalous negative polarization

It is well known that the current, which flows through 2QDs strongly depends on various parameters of the system, in particular the macroscopic capacitances C_{ij} and the resistances R_{ij} . The capacitances C_{ij} determine the charging energies of the individual quantum dots E_1^{ch} , E_2^{ch} and their electrostatic coupling energy E_{12}^{ch} , while resistances R_{ij} are responsible for the current intensity.

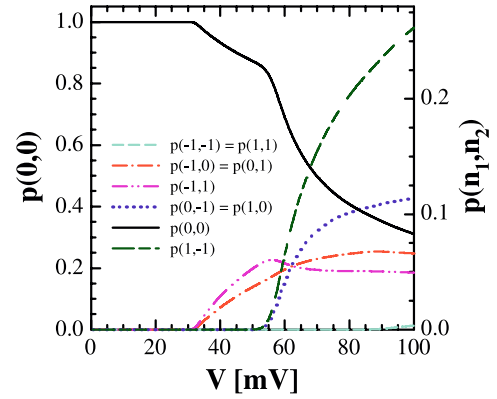


Figure 3. Voltage dependence of the probabilities $p(n_1, n_2)$ for the states, which are relevant to transport. The parameters are the same as in figure 2.

In this section we consider a symmetrical system with the capacitance $C_{L1} = C_{2R}$ and the resistance $R_{L1} = R_{2R}$. In addition we assume that R_{12} is larger than R_{L1} and $R_{12}/R_{L1} = 5$. Figure 2(a) shows the current–voltage characteristic for our system. For small voltages, the current cannot flow through the 2QDs device due to the Coulomb blockade effect. The current starts to flow above a threshold voltage $V_1^{\text{th}} \approx 32 \text{ mV}$. The current monotonically grows with increasing bias voltage V . The small bend, one can see in the I – V characteristic, is due to opening of new transport channels.

Intuition suggests that with increasing V QD1 should be monotonically charged by electrons (because $R_{L1} < R_{12}$), while electrons from QD2 should outflow (because $R_{12} > R_{2R}$). However, figure 2(b) shows that QDs are charged non-monotonically. At the threshold voltage V_1^{th} , electrons start to outflow from QD1, so the corresponding charge accumulation decreases ($\langle n_1 \rangle < 0$, see figure 2(b)). At the same time electrons are accumulated on QD2, so $\langle n_2 \rangle > 0$ (see figure 2(b)). This causes negative polarization $P = \langle n_1 - n_2 \rangle$. For higher voltages, above V_2^{th} , the charge accumulation on QD1 increases monotonically, while that on QD2 monotonically decreases (see figure 2(b)). Then, the polarization P switches from a negative to a positive value for $V^{\text{switch}} > V_2^{\text{th}}$. Simultaneously the charge accumulations $\langle n_i \rangle$ also change sign. Moreover, in the steady state, the average potential drop $\langle V_{L1} \rangle$ on the junction L1 should be the same as the average potential drop $\langle V_{2R} \rangle$ on the junction 2R, because of the symmetry of the system. So, one can find from equations (1)–(3) that the charge accumulations $\langle n_1 \rangle$ and $\langle n_2 \rangle$ fulfil condition $\langle n_1 \rangle = -\langle n_2 \rangle$, the total charge accumulation $Q = \langle n_1 + n_2 \rangle = 0$ and the polarization $P = 2\langle n_1 \rangle$ for any V .

To explain the polarization switching effect presented in figure 2 we performed analysis of the occupation probabilities $p(n_1, n_2)$ versus the bias voltage V . One can see from figure 3, that for small voltages $V < V_1^{\text{th}}$, the probability $p(0, 0)$ that both dots are empty is equal to one, and current cannot flow through the system. When the voltage exceeds the threshold voltage V_1^{th} then the current I begins to flow through the system. The probabilities $p(0, 1)$, $p(-1, 0)$ and $p(-1, 1)$ rise, which result from opening new charge channels $(0, 1)$,

$(-1, 0)$ and $(-1, 1)$, respectively. These states correspond to the condition $n_2 > n_1$, so electronic transport through them is responsible for the negative polarization seen in figure 2(b). When the voltage exceeds V_2^{th} new transport channels (with $n_1 > n_2$) $(1, 0)$, $(0, -1)$ and $(1, -1)$ are opened. It is clearly seen in figure 3 as an increase of the probabilities $p(1, 0)$, $p(0, -1)$ and $p(1, -1)$. Hence, states $(1, 0)$, $(0, -1)$ and $(1, -1)$ are responsible for the positive polarization P . For bias voltages higher than V^{switch} the states $(1, 0)$, $(0, -1)$ and $(1, -1)$ are favoured, which leads to the increase of the polarization P above zero (see figure 2(b)). In figure 2 one can also see an intense change of the polarization around V_3^{th} . This effect is due to opening of new charge channels, e.g. $(1, -2)$, $(2, -1)$ and $(2, -2)$. The new charge states also give positive contribution to the polarization P . It is worth noting, that due to the symmetry of the system, $p(-1, -1) = p(1, 1)$, $p(-1, 0) = p(0, 1)$ and $p(0, -1) = p(1, 0)$, see figure 3.

Let us now analyse microscopic processes, which are responsible for the non-monotonic behaviour of the polarization P seen in figure 2(b). Transport through the 1D array of quantum dots occurs when the free energy difference ΔF_{ij} of each tunnelling event in the sequence (which transfer an electron from one electrode to another) is positive. For example, to transfer an electron from the left to the right electrode through 2QDs system three free energy differences have to be positive: $\Delta F_{L1}(n_1, n_2; n_1 + 1, n_2)$, $\Delta F_{12}(n_1 + 1, n_2; n_1, n_2 + 1)$ and $\Delta F_{2R}(n_1, n_2 + 1; n_1, n_2)$. These free energy differences correspond to threshold voltages $V_{L1}^{\text{th}}(n_1, n_2; n_1 + 1, n_2)$, $V_{12}^{\text{th}}(n_1 + 1, n_2; n_1, n_2 + 1)$ and $V_{2R}^{\text{th}}(n_1, n_2 + 1; n_1, n_2)$, which can be calculated from conditions $\Delta F_{ij}(n_1, n_2; n'_1, n'_2) = 0$. So, one can say that the particular sequence of tunnelling events is activated for the threshold voltage:

$$V^{\text{th}} = \max\{V_{L1}^{\text{th}}(n_1, n_2; n_1 + 1, n_2), V_{12}^{\text{th}}(n_1 + 1, n_2; n_1, n_2 + 1), V_{2R}^{\text{th}}(n_1, n_2 + 1; n_1, n_2)\}. \quad (10)$$

Equation (10) has been derived for the sequence, in which at first one electron jumps from the left electrode to the QD1. However, one can obtain similar formulae for other sequences, e.g. when at first an electron is transferred through junction 12 between dots. We have found, from equation (10) for this sequence, that the threshold voltage $V_1^{\text{th}} = -e(1/C_{L1} + 1/C_{2R})/2 \approx 32$ mV is determined by the free energy difference $\Delta F_{12}(0, 0; -1, 1)$. This means, that an electron can be transferred through the tunnel junction 12 from the QD1 to the QD2 with tunnelling rate $\Gamma_{12}(0, 0; -1, 1)$. One can say that a new charge channel $(-1, 1)$ is activated and available for the tunnelling events, which is seen in figure 3 as a rapid increase of the occupation probability $p(-1, 1)$ at $V = V_1^{\text{th}}$. Moreover, because the free energy difference $\Delta F_{21}(-1, 1; 0, 0)$ is negative for $V > V_1^{\text{th}}$, the reverse processes, in which an electron is transferred from QD2 to QD1, vanish (i.e. $\Gamma_{21}(-1, 1; 0, 0) \rightarrow 0$ for $V > V_1^{\text{th}}$). Further, because the free energy differences $\Delta F_{L1}(-1, 1; 0, 1)$ and $\Delta F_{2R}(-1, 1; -1, 0)$ are positive, the occupation probabilities $p(0, 1)$ and $p(-1, 0)$ rise (see figure 3), so additional two transport channels $(0, 1)$ and $(-1, 0)$ open at V_1^{th} . It means

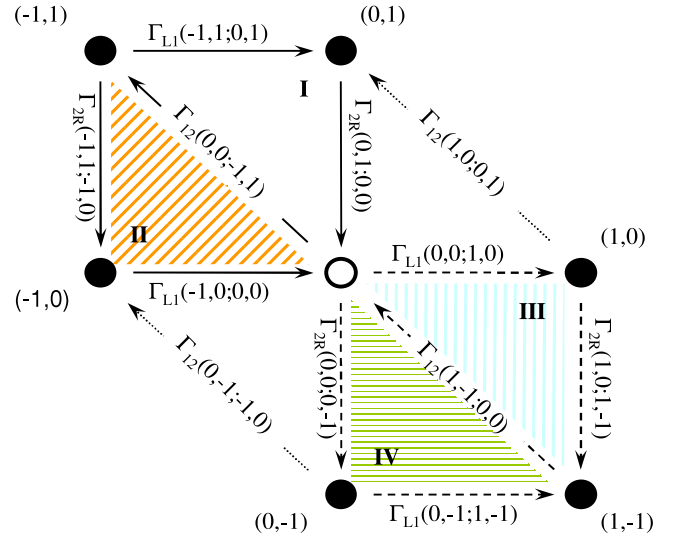


Figure 4. 2D space of states (n_1, n_2) contributing to transport and polarization at low and moderate voltages V . Black points denote available channels. Equilibrium $(0, 0)$ is marked by O. Arrows show relevant tunnelling processes $\Gamma_{ij}(n_1, n_2; n'_1, n'_2)$ between initial (n_1, n_2) and final (n'_1, n'_2) states. The paths are numbered by I, II (stroke lines), III (vertical lines), IV (horizontal lines). The picture is related to figure 3.

that in the second step either an electron can tunnel from the left electrode to the QD1 (through the junction L1) with the rate $\Gamma_{L1}(-1, 1; 0, 1)$ or an electron from the QD2 will jump to the right electrode (through the junction 2R) with the rate $\Gamma_{2R}(-1, 1; -1, 0)$. In the last step of the sequence, the system returns to its initial state $(0, 0)$. It can be done via an electron tunnelling (with the rate $\Gamma_{2R}(0, 1; 0, 0)$) through the junction 2R from QD2 to the right electrode or via an electron transfer (with the rate $\Gamma_{L1}(-1, 0; 0, 0)$) from the left electrode to QD1. Summarizing, above V_1^{th} one electron can be transferred from the left to the right electrode over the sequence of the following tunnelling processes (denoted by \rightarrow), which couple adjacent states in the 2D space of states (n_1, n_2) : $(0, 0) \rightarrow (-1, 1) \rightarrow (0, 1) \rightarrow (0, 0)$ or $(0, 0) \rightarrow (-1, 1) \rightarrow (-1, 0) \rightarrow (0, 0)$, see path I and II in figure 4 (solid lines). Both sequences give a negative contribution to the polarization P . It is worth noting, that the process $\Gamma_{12}(0, 0; -1, 1)$ is crucial, because it initiates both sequences shown schematically above.

The polarization P decreases up to the voltage $V_2^{\text{th}} = -e(1/C_{12} + 1/C_{2R})/2 \approx 56$ mV (see figure 2) when the new channels $(1, 0)$, $(0, -1)$ and $(1, -1)$ open (see figure 3). The threshold voltage V_2^{th} is determined similarly to V_1^{th} . We have calculated free energy differences and found that $\Delta F_{L1}(0, 0; 1, 0)$ and $\Delta F_{2R}(0, 0; 0, -1)$ become positive at the threshold voltage V_2^{th} while $\Delta F_{21}(0, 0; 1, -1)$ is negative. It means that at first an electron from the left electrode can tunnel to QD1 (with the rate $\Gamma_{L1}(0, 0; 1, 0)$) or an electron from QD2 will be transferred to the right electrode (with the rate $\Gamma_{2R}(0, 0; 0, -1)$). In addition, above V_2^{th} both backward processes $\Gamma_{1L}(1, 0; 0, 0)$ and $\Gamma_{R2}(0, -1; 0, 0)$ vanish, so an electron cannot simply return from the states $(1, 0)$ and $(0, -1)$ to the ground state $(0, 0)$. In the next step, either an electron from QD2 will tunnel (with the rate $\Gamma_{2R}(1, 0; 1, -1)$) to

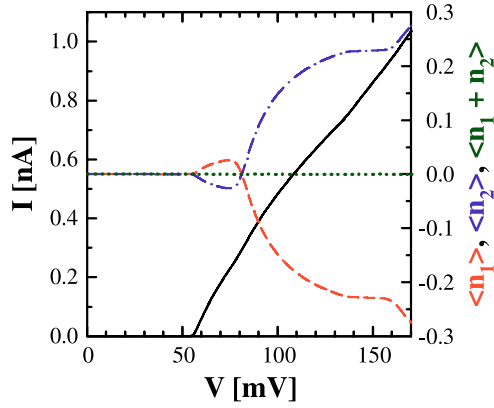


Figure 5. Voltage dependence of the current (solid curve), the charge accumulations on QD1— $\langle n_1 \rangle$ (dash curve), QD2— $\langle n_2 \rangle$ (dash-dot curve) and the total charge accumulated on the system— $\langle n_1 + n_2 \rangle$ (dot curve). The polarization $P = 2\langle n_1 \rangle$. The parameters are: $R_{L1} = R_{2R} = 50 \text{ M}\Omega$, $R_{12} = 10 \text{ M}\Omega$, $C_{L1} = C_{2R} = 2 \text{ aF}$, $C_{12} = 5 \text{ aF}$, $V_L = 0$, $V_R = V$, $T \approx 2.32 \text{ K}$.

the right electrode through the junction $2R$ or an electron from the left electrode can be transferred (with the rate $\Gamma_{L1}(0, -1; 1, -1)$) to QD1 through the junction $L1$. At the end, the system can return from the state $(1, -1)$ to the initial state $(0, 0)$, (with the rate $\Gamma_{12}(1, -1; 0, 0)$). In the case one electron can be transferred from the left to the right electrode over the sequence of the following tunnelling processes (denoted by \rightarrow): $(0, 0) \rightarrow (1, 0) \rightarrow (1, -1) \rightarrow (0, 0)$ or $(0, 0) \rightarrow (0, -1) \rightarrow (1, -1) \rightarrow (0, 0)$, see path III and IV in figure 4 (dash lines). Since, these two sequences give a positive contribution to P , the polarization starts to increase for voltages higher then V_2^{th} . Moreover, for $V > V^{\text{switch}}$ the sequences, which give positive contribution to the polarization are preferable and total polarization P become positive. It is worth noting, that at V^{switch} , when switching of polarization occurs, new channels are not open. The effect is due to competition between different tunnelling rates.

Apart from the polarization switching from negative to positive values (seen in figure 2(b)) we have found an inverse effect, when the polarization P changes its sign from positive to negative. This situation is presented in figure 5, where the inverse change of polarization is correlated with reverse behaviour of accumulated charges $\langle n_1 \rangle$ and $\langle n_2 \rangle$. The effect can be analysed in a similar way. One can find the first threshold voltage from the equation (10). In the case, the first threshold voltage is determined by the free energy difference $\Delta F_{L1}(0, 0; 1; 0) = \Delta F_{2R}(0, 0; 0; -1)$ and it is $V_1^{\text{th}} = -e(1/C_{12} + 1/C_{2R})/2$. It means that at first, channels $(1, 0)$ and $(0, -1)$ are activated and transport occurs through sequences shown schematically by dashed lines in figure 4. Now, the effect of the dynamical switching of polarization occurs when charging energies $E_1^{\text{ch}}, E_2^{\text{ch}} \approx 46.7 \text{ mV}$ are larger than the coupling energy $E_{12}^{\text{ch}} \approx 33.4 \text{ mV}$. However, the resistance of the dot-dot tunnel barrier is smaller than resistances of the dot-electrode, $R_{12}/R_{L1(2R)} = 0.2$. For high bias voltages the polarization decreases and achieves a large negative value. This means, that in the high voltage range, more electrons are localized on QD2 than on QD1.

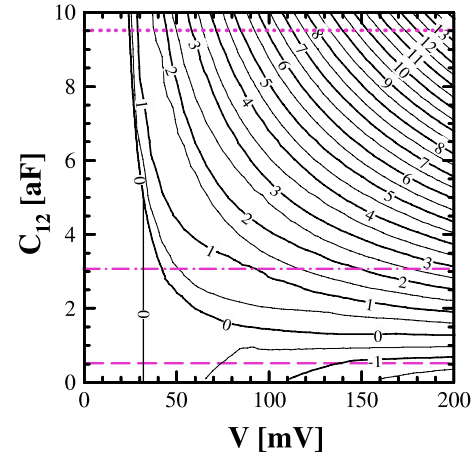


Figure 6. Contour plot of the polarization $P = \langle n_1 - n_2 \rangle$ as a function of the bias voltage V and the dot-dot capacitance C_{12} . The other parameters are the same as those in figure 2.

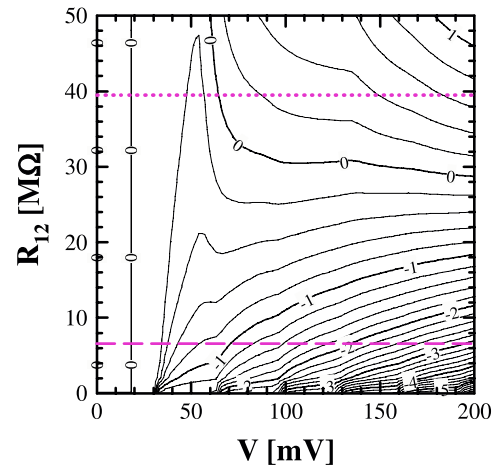


Figure 7. Contour plot of the polarization $P = \langle n_1 - n_2 \rangle$ as a function of the bias voltage V and the dot-dot resistance R_{12} . The other parameters are the same as those in figure 2.

This effect of charge accumulation is due to the asymmetry between R_{12} and R_{L1}, R_{2R} . However, for smaller voltages $V_1^{\text{th}} < V < 80 \text{ mV}$ the charge accumulation is reversed, i.e. more additional electrons are localized on QD1 than on QD2.

The results presented in figures 2 and 5 have been calculated for quite different, but particular sets of macroscopic capacitances C_{ij} and resistances R_{ij} . It is also interesting to know how the DPS effect depends on the coupling energy E_{12}^{ch} (on C_{12}) or transparency of the dot-dot tunnel barrier (related with R_{12}). The results of our computations are shown on the contour plots in figures 6 and 7. It is obvious that the electrostatic coupling energy E_{12}^{ch} increases with an increase of C_{12} , while the both charging energies E_1^{ch} and E_2^{ch} decrease. However, always $E_{12}^{\text{ch}} < E_1^{\text{ch}}, E_2^{\text{ch}}$. For small $C_{12} \ll C_{L1}, C_{2R}$ (e.g. for the dashed line in figure 6) the polarization is always negative and decreases monotonically with an increase of V , while for large $C_{12} \gg C_{L1}, C_{2R}$ (e.g. for the dotted line in figure 6) the polarization is always positive

and monotonically increases with V . The non-monotonic behaviour of the polarization occurs (e.g. for the dash-dot line in figure 6) for values of C_{12} , which belong to the narrow interval $1.75 \text{ aF} < C_{12} < 3.75 \text{ aF}$. It means that the effect of DPS is suppressed for very small or very large electrostatic dot-dot couplings. It is worth noting, that in this case, the resistance of the dot-dot barrier $R_{12} = 50 \text{ M}\Omega$ is larger than the dot-electrode resistances $R_{L1} = R_{2R} = 10 \text{ M}\Omega$.

Next, we study how the change of the dot-dot resistance R_{12} influences the polarization. It is assumed that now all capacitances are constant and $C_{L1} = C_{2R} = 5 \text{ aF}$, $C_{12} = 2 \text{ aF}$. The results are presented in figure 7. One can see that for resistance R_{12} up to $\approx 30 \text{ M}\Omega$ the polarization is always negative (e.g. if one follows the dashed line in figure 7). For higher values of R_{12} the polarization changes non-monotonically from negative to positive values (e.g. for the dotted line in figure 7). Because R_{ij} does not have any influence on the threshold voltages, the width of the negative polarization region as a function of voltage is almost constant for large $R_{12} \gg R_{L1}, R_{2R}$. However, with an increase of R_{12} the intensity of the negative polarization decreases. The results presented in figure 7 depend on the competition between tunnelling through channels with a positive and a negative contribution to the polarization. The channels with positive contribution to the polarization P dominate only for large $R_{12} \gg R_{L1}, R_{2R}$ and large V . For small $R_{12} \ll R_{L1}, R_{2R}$ the channels contributing to negative polarization are more strongly activated over the voltage range.

It is worth noting that temperature can also strongly affect the polarization of the system. For example we will analyse the influence of the temperature on the results presented in figure 2. One can find from equation (6), that for very low temperature T ($k_B T \ll E_i^{\text{ch}}$), the tunnelling rate $\Gamma_{12}(0, 0, -1, 1)$ abruptly rises at the threshold voltage V_1^{th} (when a new transport channel $(-1, 1)$ is opened). Because for $V < V_2^{\text{th}}$ the channels contributing to the positive polarization are closed, the polarization is negative for voltages $V_1^{\text{th}} < V < V_2^{\text{th}}$. For higher temperatures ($k_B T < E_i^{\text{ch}}$) the tunnelling rates (e.g. $\Gamma_{L1}(0, 0, 1, 0)$ and $\Gamma_{2R}(0, 0, 0, -1)$) increase smoothly as a function of bias voltage. It means, that the channels contributing to positive polarization are also opened below V_2^{th} . This leads to suppression of the negative polarization for $V < V_2^{\text{th}}$. Moreover, for sufficiently large temperatures ($k_B T$ is of the order of E_i^{ch}), the channels contributing to the positive polarization dominate over the whole voltage range, so the positive polarization also appears for $V < V_2^{\text{th}}$.

4. Final remarks

In the paper the dynamical (bias voltage dependent) charging effects in the 2QDs devices in the limit of sequential tunnelling have been analysed. We have found that the dynamical polarization switching (DPS), i.e. inversion of the polarization of the system, when the bias voltage increases, can occur in these systems. The effect is a result of the competition between tunnelling through different charge channels. If

the capacitances $C_{L1}, C_{2R} > C_{12}$ then the threshold voltage $V_1^{\text{th}} < V_2^{\text{th}}$, which means that for voltages $V_1^{\text{th}} < V < V_2^{\text{th}}$ the current flow through the system is mainly due to the activation of the state $(-1, 1)$, and in part through the states $(-1, 0)$ and $(0, 1)$ (see figure 4, paths I and II). In this case the polarization of the system is negative. For higher voltages $V_2^{\text{th}} < V$, the tunnelling processes through the states $(1, -1)$, $(1, 0)$ and $(0, -1)$ are activated (see figure 4, paths III and IV), which give a positive contribution to the polarization P . These two processes compete with each other. Depending on the relation of the interdot resistance R_{12} to the tunnel resistances R_{L1}, R_{2R} and on relations between the corresponding tunnelling rates $\Gamma_{ij}(n_1, n_2; n'_1, n'_2)$, the positive or the negative polarization can dominate. For $R_{12} \gg R_{L1}, R_{2R}$ the channels with positive polarization are more strongly activated and dominate for large voltages, which results in polarization switching. For small $R_{12} \ll R_{L1}, R_{2R}$ the channels contributing to negative polarization dominate in the whole voltage range.

Our analysis was performed for the symmetrical situation, when couplings of 2QDs to the both electrodes are the same ($C_{L1} = C_{2R}$, $R_{L1} = R_{2R}$). The DPS effect will also occur in asymmetrical systems. First of all, for the asymmetric capacitance coupling to the electrodes a nonzero charge accumulation $Q = \langle n_1 + n_2 \rangle \neq 0$ can appear. Tunnelling processes presented in figure 4, contributing to the current and polarization, are now different. For example the path I: $(0, 0) \rightarrow (-1, 1) \rightarrow (0, 1) \rightarrow (0, 0)$ and the path II: $(0, 0) \rightarrow (-1, 1) \rightarrow (-1, 0) \rightarrow (0, 0)$ are not equivalent. However, according to equation (10) both paths are activated at the same threshold voltage V_1^{th} , because the threshold voltage is determined by $V_1^{\text{th}} \equiv V_1^{\text{th}} = V_{\text{II}}^{\text{th}} = V_{12}^{\text{th}}(0, 0; -1, 1) = -e(1/C_{L1} + 1/C_{2R})/2$, and is not sensitive to the asymmetry between C_{L1} and C_{2R} . The situation is quite different for processes with positive polarization. The path III: $(0, 0) \rightarrow (1, 0) \rightarrow (1, -1) \rightarrow (0, 0)$ and the path IV: $(0, 0) \rightarrow (0, -1) \rightarrow (1, -1) \rightarrow (0, 0)$ are activated at different threshold voltages, namely at $V_{\text{III}}^{\text{th}} = V_{L1}^{\text{th}}(0, 0; 1, 0) = -e(1/C_{12} + 1/C_{2R})/2$ and $V_{\text{IV}}^{\text{th}} = V_{2R}^{\text{th}}(0, 0; 0, -1) = -e(1/C_{L1} + 1/C_{12})/2$, respectively. The resistances R_{L1}, R_{12}, R_{2R} (and the corresponding tunnelling rates $\Gamma_{L1}, \Gamma_{12}, \Gamma_{2R}$) are responsible for the activation strength of these processes. The DPS effect can occur in this case as well, but the voltage dependence of the polarization is more complex.

In the above presentation we have neglected the effect of gate voltages V_{G1} and V_{G2} , which can be applied to the QD1 and QD2. The polarization effects have been also studied taking into account V_{G1} and V_{G2} and modifying appropriate formulae for the voltage drops, the free energy and the tunnelling rates. The results are qualitatively the same as presented above. The threshold voltage V_1^{th} increases with increasing gate voltage V_{G1} applied to the QD1, while decreases when the gate voltage V_{G2} is applied to the QD2. We have found, that the threshold voltage $V_{\text{III}}^{\text{th}}$ always decreases, while $V_{\text{IV}}^{\text{th}}$ always increases with V_{G1} and V_{G2} .

Similar polarization effects can be found in coherent electronic transport through 2QDs [25]. The authors were not

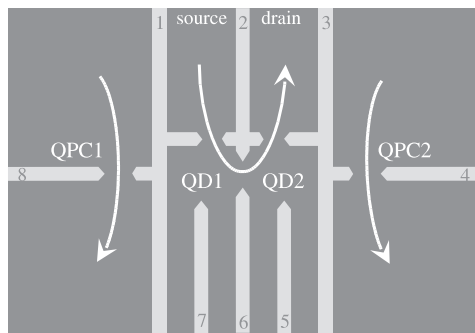


Figure 8. Scheme of a lateral 2QDs device defined by metal surface electrodes 1–8. The electrodes 1 and 2 define the tunnel junction L1 in our model, whereas the electrodes 2 and 6 define the tunnel junction 2R. The gate electrodes 5 and 7 are used to change the number of electrons on QDs. The electrodes 4 and 7 create the quantum point contacts.

interested in the DPS effect, but from their analytical formulae for the polarization, derived in the limit of weak coupling with the electrodes (see appendix in [25]), we can conclude that the DPS effect in that system is due to competition of the cohesive energy, the interdot and intradot Coulomb interactions, as well as a charge displacement due to a potential drop along the system.

Our prediction of the DPS effect can be verified experimentally. Figure 8 presents a scheme of the system of 2QDs coupled with two quantum point contacts (QPCs), which can be used as a sensible charge sensor for the DPS effect. Similar systems were used already in charge sensing experiments by many groups [1, 6, 32, 33]. Changes of the polarization P accompany changes of the conductance in quantum point contacts QPC1 and QPC2. QPCs are capacitively coupled with the quantum dots, so charge accumulated on the quantum dots strongly influences conductance of the QPCs. Thereby the proposed device gives a possibility to verify our predictions concerning the dynamical polarization switching effect.

Acknowledgments

The work was supported as part of the European Science Foundation EUROCORES Programme FoNE by funds from the Ministry of Science and Higher Education and EC 6FP (contract No. ERAS-CT-2003-980409), and the EC project RTNNANO (contract No. MRTN-CT-2003-504574).

References

- [1] Hanson R, Kouwenhoven L P, Petta J R, Tarucha S and Vandersypen L M K 2007 *Rev. Mod. Phys.* **79** 1217
- [2] van der Wiel W G, De Franceschi S, Elzerman J M, Fujisawa T, Tarucha S and Kouwenhoven L P 2003 *Rev. Mod. Phys.* **75** 1
- [3] Ono K, Austing D G, Tokura Y and Tarucha S 2002 *Science* **297** 1313
- [4] Moraru D, Ono Y, Inokawa H and Tabe M 2007 *Phys. Rev. B* **76** 075332
- [5] Johnson A C, Petta J R, Marcus C M, Hanson M P and Gossard A C 2005 *Phys. Rev. B* **72** 165308
- [6] Petta J R, Johnson A C, Marcus C M, Hanson M P and Gossard A C 2004 *Phys. Rev. Lett.* **93** 186802
- [7] Liu H W, Fujisawa T, Hayashi T and Hirayama Y 2005 *Phys. Rev. B* **72** 161305
- [8] Pothier H, Lafarge P, Urbina C, Esteve D and Devoret M H 1992 *Europhys. Lett.* **17** 249
- [9] Iñarrea J, Platero G and MacDonald A H 2007 *Phys. Rev. B* **76** 085329
- [10] Weymann I and Barnaś J 2006 *Phys. Rev. B* **73** 033409
- [11] Aguiar-Hualde J M, Chiappe G and Louis E 2007 *Phys. Rev. B* **76** 085314
- [12] Muralidharan B and Datta S 2007 *Phys. Rev. B* **76** 035432
- [13] Pedersen J N, Lassen B, Wacker A and Hettler M H 2007 *Phys. Rev. B* **75** 235314
- [14] Weymann I 2007 *Phys. Rev. B* **75** 195339
- [15] Michałek G and Bułka B R 2006 *Eur. Phys. J. B* **52** 411
- [16] Likharev K K 1999 *Proc. IEEE* **87** 606
- [17] Loss D and DiVincenzo D P 1998 *Phys. Rev. A* **57** 120
- [18] Roloff R and Pötz W 2007 *Phys. Rev. B* **76** 075333
- [19] Hartmann U and Wilhelm F K 2007 *Phys. Rev. B* **75** 165308
- [20] Stepanenko D and Burkard G 2007 *Phys. Rev. B* **75** 085324
- [21] Lambert N, Aguado R and Brandes T 2007 *Phys. Rev. B* **75** 045340
- [22] Sindel M, Silva A, Oreg Y and von Delft J 2005 *Phys. Rev. B* **72** 125316
- [23] Michałek G and Bułka B R 2002 *Eur. Phys. J. B* **28** 121
- [24] König J and Gefen Y 2005 *Phys. Rev. B* **71** 201308
- [25] Kostyrko T and Bułka B R 2003 *Phys. Rev. B* **67** 205331
- [26] Melsen J A, Hanke U, Müller H-O and Chao K-A 1997 *Phys. Rev. B* **55** 10638
- [27] Amman M, Wilkins R, Ben-Jacob E, Maker P D and Jaklevic R C 1991 *Phys. Rev. B* **43** 1146
- [28] Beenakker C W J 1991 *Phys. Rev. B* **44** 1646
- [29] Schön G 1998 *Quantum Transport and Dissipation* ed T Dittrich, P Hänggi, G-L Ingold, B Kramer, G Schön and W Zwerger (New York: Wiley-VCH) p 149
- [30] Averin D V, Korotkov A N and Likharev K K 1991 *Phys. Rev. B* **44** 6199
- [31] Grabert H and Devoret M H (ed) 1992 *Single Charge Tunneling (NATO Advanced Study Institute, Series B: Physics vol 294)* (New York: Plenum)
- [32] Elzerman J M, Hanson R, Greidanus J S, Willems van Beveren L H, De Franceschi S, Vandersypen L M K, Tarucha S and Kouwenhoven L P 2003 *Phys. Rev. B* **67** 161308
- [33] DiCarlo L, Lynch H J, Johnson A C, Childress L I, Crockett K, Marcus C M, Hanson M P and Gossard A C 2004 *Phys. Rev. Lett.* **92** 226801